In-situ Soil Moisture Sensing: Measurement Scheduling and Estimation using Compressive Sensing

Xiaopei Wu
School of Computer Science and Engineering
Univ. Electronic Science and Technology of China
Department of Electrical Engineering and Computer Science, Univ. of Michigan
wuxiaopei84@gmail.com

Mingyan Liu*
Department of Electrical Engineering and Computer Science
University of Michigan, Ann Arbor
mingyan@eecs.umich.edu

ABSTRACT

We consider the problem of monitoring soil moisture evolution using a wireless network of in-situ underground sensors. To reduce cost and prolong lifetime, it is highly desirable to rely on fewer measurements and estimate with higher accuracy the original signal (soil moisture temporal evolution). In this paper we explore results from the compressive sensing (CS) literature and examine their applicability to this problem. Our main challenge lies in the selection of two matrices, the measurement matrix and a representation basis. The physical constraints of our problem make it highly non-trivial to select these matrices, so that the latter can sufficient sparsify the underlying signal while at the same time be sufficiently incoherent with the former, two common pre-conditions for CS techniques to work well. We construct a representation basis by exploiting unique features of soil moisture evolution. We show that this basis attains very good tradeoff between its ability to sparsify the signal and its incoherence with measurement matrices that are consistent with our physical constraints. Extensive numerical evaluation is performed on both real, high-resolution soil moisture data and simulated data, and through comparison with a closed-loop scheduling approach. Our results demonstrate that our approach is extremely effective in reconstructing the soil moisture process with high accuracy and low sampling rate.

Categories and Subject Descriptors

I.6.m [**SIMULATION AND MODELING**]: Miscellaneous

General Terms

Performance, Measurement

*Corresponding Author

IPSN'12, April 16–20, 2012, Beijing, China.

Keywords

Measurements Scheduling, Compressive Sensing, Soil Moisture Sensing

1. INTRODUCTION

This paper studies the efficient measurement scheduling and sensing of soil moisture. Soil moisture is a critical data type and measurement need in many scientific applications. For instance, it is used in all land surface models, water and energy balance models, weather prediction models, general circulation models, and ecosystem process simulation models [1]. It is also a key measurement need in precision farming and agricultural drought monitoring.

Soil moisture data has traditionally been collected using remote sensing techniques like radars and radiometers onboard satellites. Remote sensing covers large areas, but produces very coarse grained measurements, on the order of square kilometers. It was not until recently, with the advances in integrated wireless communication, sensing and processing technology, has in-situ sensing become a feasible option [2, 3]. In-situ moisture sensors can be densely deployed over a region of interest, at a resolution of one in every few square-feet, and thus can produce much finer grained measurements. To collect desired data at a single location, soil moisture sensor probes are typically placed vertically under the ground at different depths, up to 2 meters deep, with wires connecting them to a ground actuation and wireless transceiver module, see e.g., the SoilScape project [4][1]. This wireless node actuates the moisture probes to take measurements and transfers the collected data wirelessly to a remote central location or base station for processing; an example of such a network is described in more detail in [4].

To gather sufficient information on the temporal and spatial variations and characteristics of soil moisture, it is highly desirable to deploy moisture probes (and the associated wireless nodes) at sufficiently high density, and to take measurements at sufficiently high frequency. A competing objective is to have the network function in a unmanned fashion for as long as possible, since such networks are typically deployed in an open (sometimes remote) field without immediate access to power or human intervention. This requires us to

[1]Similar and alternative instrumentations have been used in other studies such as the Suelo project [3], which targets the monitoring of soil which includes but is not specifically designed for moisture data collection.

reduce the working times of the wireless nodes to conserve energy, even when renewable sources are used.

For a single wireless node, these competing interests imply that we need to make judicious decisions in measurement scheduling, i.e., when is the best time to take a measurement, so as to minimize the total amount of time the node needs to be active in actuating the moisture probes and in data transmission, while still satisfying the monitoring objective, i.e., achieving a desired level of accuracy in the estimated soil moisture evolution using the measurement data collected. In this paper we examine how compressive sensing and sparse sampling theory may be used to achieve these goals. Note that such measurement scheduling in general runs parallel to other energy efficient methods one may wish to adopt, including MAC and routing. It can also be jointly designed with a node's sleep schedules.

This problem belongs to the larger class of sensor scheduling problems. There are two general approaches. The first is a closed-loop approach that makes a measurement decision using past observations and decisions. This typically requires the knowledge of prior statistics of the underlying random process to be monitored, gained either through assumption or training, and is also sometimes referred to as the Bayesian approach; examples include [5, 6, 7, 8, 9, 10, 11, 12, 13, 14], with [10] focusing specifically on monitoring soil moisture.

The second is an open-loop approach whereby measurement decisions are made independent of past observations and decisions. Compressive sensing based measurement falls under this category. Recent advances in compressive sensing (CS) theory [15, 16, 17] allow one to represent compressible/sparse signals with significantly fewer samples than required by the Nyquist sampling theorem. It is therefore particularly attractive in a resource constrained setting like ours. This technique has been used in data compression [18], channel coding [19], analog signal sensing [20], routing [21] and data collection [22], with varying degrees of success. Applied to our context, the idea would be to sample the soil moisture in time in some fashion (typically randomly) and use compressive sensing techniques to reconstruct or recover the entire process.

There are two major challenges in applying CS techniques to our problem context. (1) It is not immediately clear how to find a good representation basis (Ψ) under which the soil moisture process may be sparsely represented. There is no systematic way of selecting such a matrix; it is usually done through trials and experience. (2) Under the CS framework the measurement scheduling is specified by a measurement matrix (Φ) (see e.g., the commonly used Gaussian matrix), which is often required to be dense, i.e., each measurement corresponds to a linear combination of multiple samples [18, 21, 22]. However, in our problem the physical nature of the monitoring device is such that each measurement corresponds to one and only one sample of the underlying physical process. This makes our measurement matrix extremely sparse, a feature that often does not bode well for its success, see e.g., [21]. An additional consequence of a sparse measurement matrix Φ is that it becomes hard to make it sufficiently incoherent from Ψ, a typical condition required for the success of CS techniques. We show in subsequent sections how these challenges can be addressed.

Our main results and contributions are summarized as follows. (1) We identify a representation basis Ψ, under which the soil moisture process can be nearly sparsely represented. (2) This matrix is shown to work extremely well with a number of measurement matrices that are consistent with our application context, including those induced by random and uniform scheduling methods. (3) We further compare this approach to two non-CS based methods, a closed-loop approach and an interpolation based approach, to demonstrate its performance. In particular, the comparison with the closed-loop approach sheds light on the inherent limit of the latter. All our methods are tested using two sets of data: a real soil moisture data set collected from a botanical garden, and a simulated data set calibrated using data collected from a farm.

Even though our evaluation is based on two specific soil moisture data sets, the methodology presented in this paper is more generally applicable. Firstly, this method works well on soil moisture data from other soil types beyond the two data sets used in the study. This is because our method exploits the dynamics driven by rainfall events, which is common across all soil types. Secondly, the combination of representation basis we proposed and the recovery algorithm used can potentially work well with other signal types that are relatively smooth in nature as we note later in Section 4.2. This however must be borne out by further experiments which is out of the scope of the current paper but may be pursued in future studies. Finally, we believe the general methodology followed in this paper, i.e., the selection of a sampling method, a representation basis and a recovery algorithm, as well as verifying the sparsity and incoherence, is applicable to a broad range of similar studies that may wish to employ compressive sensing techniques. While the specific selections of these elements may vary from application to application, and is typically done through experience and trial-and-error, this study nevertheless represents as systematic as possible a scientific method that may be used by other studies.

The remainder of this paper is organized as follows. In Section 2 we describe the problem as well as the data sets we use for our study. Section 3 gives brief background information on related CS literature. In Section 4 we discuss the design of the two matrices in order to apply CS technique to our measurement scheduling problem. Numerical results are presented in Section 5, with comparison to two non-CS (closed-loop and interpolation) approaches discussed in Section 6. Section 7 concludes the paper.

2. THE SCHEDULING PROBLEM AND SOIL MOISTURE DATA

We will focus on the monitoring of soil moisture evolution at a single location, as the discussion and methodology equally applies to monitoring multiple locations. As mentioned in the introduction, typically multiple soil moisture probes are placed vertically, up to 2 meters deep underground, at a single lateral location [4]. While these probes can be activated separately, from an energy management point of view it is far more efficient to activate them all at the same time (i.e., to have them follow the same measurement schedule). This is because the processor (on the ground wireless node) needs to be on (in wake mode) in order to activate any probe, and once it is on it takes very little extra energy to activate an additional probe. For this

reason we will treat a single location as having a single measurement schedule.

We will also assume that the underlying moisture process is discrete in time. This is obviously not true, but a sufficiently good representation of reality if the time unit is small enough with respect to the time scale of change in the soil moisture, which as we shall see is not very fast. More importantly, it should be noted that since the measurement device operates in discrete time no matter how high the frequency is, the best "ground truth" data is also inevitably discrete in time as a result. Therefore to adopt a discrete time model allows us to precisely quantify the performance of our method using the best ground truth we have available.

Denote by $\mathbf{x} = \{x_t, t = 0, 1, 2, \cdots, N\}$ an actual realization of the soil moisture process. A *measurement policy* π is given by a sequence of sampling times: $T^\pi = \{t_1, t_2, \cdots, t_n\} \in \{1, 2, \cdots, N\}$. Assuming perfect measurements (no error or noise), this policy induces the following *sampled sequence* $\mathbf{x}^\pi = \{x_{t_1}, x_{t_2}, \cdots, x_{t_n}\}$. An *estimation policy* λ then takes this sampled sequence and produces estimates of the original sequence $\hat{\mathbf{x}}^\lambda = \{\hat{x}_t, t = 1, 2, \cdots, N\}$, where $\hat{x}_t = x_t$ if $t \in T^\pi$, and $\hat{x}_t = \hat{x}_t^\lambda(\mathbf{x}^\pi)$ otherwise, for some estimation function $\hat{x}_t^\lambda()$.

The objective is to select the best measurement and estimation policies so as to minimize the estimation error subject to a requirement on the average sampling rate being no more than a certain desired level:

$$\begin{aligned} \min_{\pi,\lambda} \quad & \text{Err}\left(\mathbf{x}, \hat{\mathbf{x}}^\lambda(\mathbf{x}^\pi)\right) \\ \text{s.t.} \quad & n/N \leq \alpha \ , \end{aligned}$$

where Err() is certain error measure, e.g., the mean-squared error, and α is the requirement on sampling or measurement rate.

We next discuss the moisture process $\mathbf{x}$ we use in our study. As mentioned, we will use two data sets. The first one, also referred to as the *garden data*, was collected at the Matthaei Botanical Garden at the University of Michigan, Ann Arbor ((latitude, longitude) approximately (42.300437, -83.663442)), over a 2-month period between August and October 2009. Three moisture probes were buried at depths 25mm, 67mm and 123mm, from the surface, respectively, and took measurements at the rate of once every 10 minutes. This is shown in Figure 1 in a progression of three figures, each with increasing resolution to show both a global as well as a zoomed-in view of the variation in the process.

A second data set, also referred to as the *farm data*, is a simulated one in an environment consistent with the climate and topography of Canton, Oklahoma ((latitude, longitude) approximately (36.00063,-98.63319)), over a 6-month period, between August 2010 and March 2011, at the sampling rate of one measurement per hour. This data is generated by a land surface hydrology simulation MOBIDIC [23], and has been calibrated using location- and time-specific variable exogenous forcings (e.g., rainfall, temperature, cloud cover, and solar radiation) and landscape parameters (e.g., vegetation cover, soil type, and topography), as well as actual data collected at this location. The farm data contains one depth per location; traces of 3 locations are shown in Figure 2, in a similar progression with increasing resolution.

The reason for using two different sets of data is to provide some diversity in the type of soil moisture processes we use for evaluation. We see that the soil moisture peaks shortly after a rainfall event, with the corresponding moisture level primarily determined by the precipitation. The moisture then slowly dissipates and evaporates, following a roughly monotonic non-increasing pattern. Over a period of dry weather, the soil moisture level stays relatively constant, resulting in a piece-wise smooth curve between two successive rainfall events. Except for the up-shoot at the onset of a rainfall, the moisture variation exhibits fairly high temporal correlation.

3. COMPRESSIVE SENSING

In this section we briefly summarize the part of the compressive sensing (CS) literature most relevant to the study presented in this paper.

Consider a discrete signal given by the vector $\mathbf{x}$ of size N. Results in compressive sensing [24] have shown that if $\mathbf{x}$ is sparse, i.e., if $||\mathbf{x}||_o \ll N$, then it is possible to reconstruct it from M random samples produced by a suitably chosen linear transform Φ of $\mathbf{x}$: $\mathbf{y}_{M\times 1} = \Phi\mathbf{x}$, where $M < N$. The $M \times N$ matrix Φ is usually referred to as the *measurement matrix*. In other words, we can recover signal $\mathbf{x}$ from $\mathbf{y}$ if $\mathbf{x}$ is sufficiently sparse, subject to some pre-conditions on Φ (more discussed below). In practice, $\mathbf{x}$ is usually non-sparse. However, it can often be sparsely represented in an alternative domain. Specifically, $\mathbf{x}$ may be further written as $\mathbf{x} = \Psi\mathbf{s}$, for some $N \times N$ matrix Ψ, where $\mathbf{s}$ is the $N \times 1$ coefficient vector in the Ψ-domain with $||s||_o = K$, where $K \ll N$. The matrix Ψ will also be referred to as the *representation basis*. The measurement vector can thus be written as

$$\mathbf{y} = \Phi\Psi\mathbf{s} \ , \tag{1}$$

and the associated signal recovery problem is to determine $\mathbf{s}$ for given measurement $\mathbf{y}$ and known matrices Φ and Ψ. The reconstruction of the original signal is given by $\mathbf{x} = \Psi\mathbf{s}$. Clearly, Equation (1) is an under-determined linear system, as the number of equations M is much smaller than the number of variables N (i.e., number of entries of $\mathbf{s}$). Finding the solution to this ill-conditioned system has been the subject of extensive study in recent years.

There are in general the following classes of approaches. The first class seeks $\mathbf{s}$ with the smallest l_o norm:

$$\min_{\mathbf{s}\in\mathbb{R}^N} \| \mathbf{s} \|_o \quad \text{s.t. } \mathbf{y} = \Phi\Psi\mathbf{s}. \tag{2}$$

Directly solving the above is intractable [25, 26], but fast approach exists by using smoothed l_o norm, see e.g. the SL0 method proposed in [27]. A second class of approaches bypasses the original l_o minimization problem and instead seeks to solve the l_1 norm minimization problem to reduce complexity, also known as Basis Pursuit (BP), see e.g., [28, 29]:

$$\min_{\mathbf{s}\in\mathbb{R}^N} \| \mathbf{s} \|_1 \quad \text{s.t. } \mathbf{y} = \Phi\Psi\mathbf{s}, \tag{3}$$

which can be easily solved using linear programming (LP) methods. The justification for solving (3) is that for large systems of equations, the solution to either minimization is the same [28]. Algorithms exist to solve the above problem in polynomial time, including interior-point methods; there are also faster algorithms aimed at large-scale systems, see e.g., [30, 31, 32, 27]. In addition to LP, the algorithms we will examine include Iterative Re-weighted Least Squares (IRWLS) [30], and Matching Pursuit (MP), see e.g. OMP

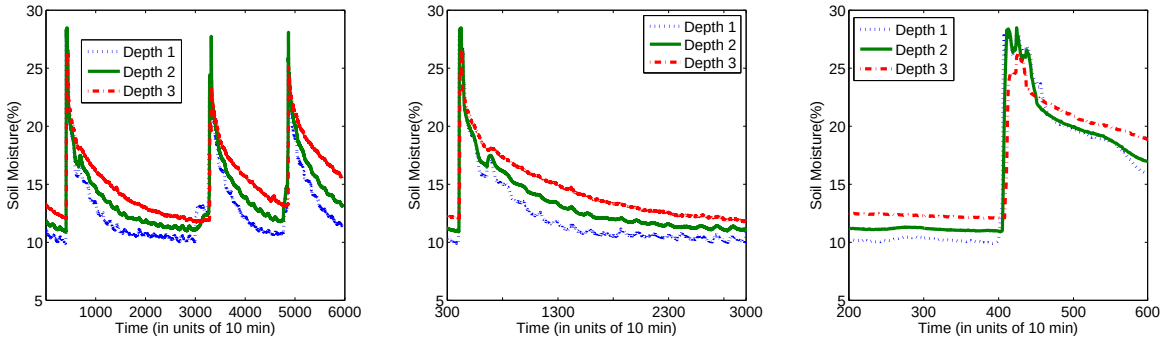

(a) Entire trace over time. (b) Variation before/after a rainfall. (c) Close-up view of a rainfall event.

Figure 1: Real soil moisture evolution collected from a botanical garden.

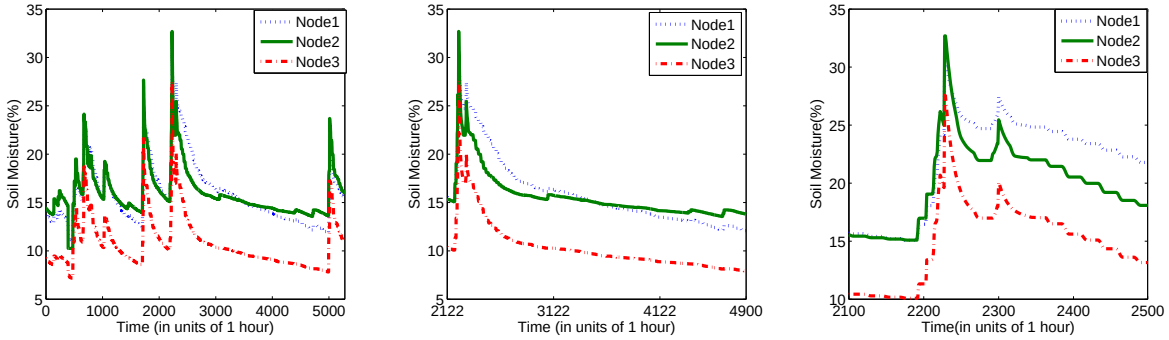

(a) Entire trace over time. (b) Variation before/after a rainfall. (c) Close-up view of a rainfall event.

Figure 2: Simulated soil moisture evolution on a farm in Oklahoma.

[31] and ROMP [32]. They are considered faster than LP but with worse estimation quality, especially if the signal is not sufficiently sparse.

Using any of the above mentioned recovery algorithm, a K-sparse signal can be reconstructed from M measurements with higher probability if M is such that:

$$M \geq C\mu^2(\Phi, \Psi)K \log N, \tag{4}$$

where C is a positive constant, N is the dimension of the signal, and $\mu(\Phi, \Psi)$ is the coherence between the two matrices Φ and Ψ. Given a pair (Φ, Ψ) of orthobases of $\mathbb{R}^N$, $\mu(\Phi, \Psi)$ can be defined as

$$\mu(\Phi, \Psi) = \sqrt{N} \max_{1 \leq i,j \leq N} | < \phi_i, \psi_j > | \in [1, \sqrt{N}]$$

where ϕ_i and ψ_j are row and column vectors of Φ and Ψ, respectively. Thus given Φ and $\mathbf{x}$, Ψ must be chosen carefully: it is desirable to represent $\mathbf{x}$ in Ψ domain sparsely (small K); at the same time, it is also desirable to have $\mu(\Phi, \Psi)$ as small as possible. The selection of Ψ to meet both criteria is in general non-trivial, especially when Φ is constrained, as we discuss next.

4. DESIGN OF MEASUREMENT AND REPRESENTATION BASIS

In this section we discuss the selection of a measurement matrix Φ and a representation basis Ψ. The measurement matrix Φ directly corresponds to a measurement scheduling policy, whereas the representation basis Ψ is used in a reconstruction algorithm so we can first determine $\mathbf{s}$ and then recover the original signal $\mathbf{x}$.

4.1 Measurement Scheduling Matrix Φ

Recall that the original soil moisture signal in time is denoted by the $N \times 1$ vector $\mathbf{x}$. The $M \times N$ measurement matrix Φ specifies a measurement scheduling policy: it contains a "1" in the (m, n) position $(1 \leq m \leq M, 1 \leq n \leq N)$ if the m-th measurement is taken at time n. The physical nature of the instrument is such that only a single measurement is taken at any scheduled time, i.e., upon actuation, the soil moisture probe takes one measurement of the soil moisture process at the time of actuation; the same point in the process cannot be measured more than once due to causality. This implies, regardless of the schedule, Φ contains one and only one "1" element in any row, and at most one "1" in any column, and "0" everywhere else.

As $M < N$, there will be exactly $N - M$ empty (all-0) columns, making the Φ matrix extremely sparse. This is very different from what is commonly studied in the literature, e.g., the Gaussian measurement matrix which is very dense with virtually no 0-entries. This poses a significant challenge, since in general the measurement matrix is required to be dense with at least one non-zero entry in each column [24, 15]. This same challenge also arose in a routing problem studied in [21], where the authors reported less

than satisfying results due to the difficulty in finding the right Ψ matrix to match the highly constrained Φ matrix.

With the above constraint in mind, we will consider two types of schedules. The first has periodic sampling times, where measurements are taken at intervals of $\lfloor \frac{N}{M} \rfloor$ discrete units of time; this will also be referred to as the *uniform schedule* (US), and the corresponding matrix denoted as Φ_U. The second follows random sampling times generated using certain probability distribution with an average sampling rate of M/N; this will be referred to as the *random schedule* (RS), and the corresponding matrix denoted as Φ_R. Note that since N is not always an integer multiple of M, in such cases under the uniform schedule the first measurement point is randomly selected within a small range $[1, \lfloor \frac{N}{M} \rfloor]$, with subsequence measurements taken every $\lfloor \frac{N}{M} \rfloor$ time units till we exhaust N.

The reason we consider these two relatively simple schedules is due to their ease in implementation. We do compare their performance with more complex schedules (see below and the closed-loop scheduling in Section 6). As we shall see the estimation accuracy of our method turns out to be highly robust against the measurement schedule.

For comparison purposes, we will also consider the commonly studied Gaussian scheduling (GS) matrix Φ_G mentioned above. It should be emphasized that this matrix is *not* practical in our scenario: since each row in this matrix has typically many non-zero entries, it requires each measurement be a linear combination of multiple samples from the soil moisture process. More importantly, as there are virtually no empty columns, this matrix essentially requires the collection of nearly all samples of the original signal. This obviously defeats our basic objective of minimizing the amount of measurements taken.

4.2 Representation Basis Ψ

As mentioned, there are two main criteria in selecting a good representation basis Ψ: (1) its corresponding inverse has to sufficiently sparsify the signal $\mathbf{x}$, and (2) it has to be sufficiently incoherent with the measurement matrix Φ. This is highly non-trivial due to the sparse nature of our Φ matrix. In general the basis Ψ can be generated without assuming a priori knowledge of the signal, other than its size (which determines the size of the matrix). However, to generate a basis that meets the above two criteria without exploiting any feature of the signal can take a large amount of trial-and-error. Thus typically certain known features of the signal are taken into account in searching for a suitable basis to speed up this design process.

To this end, we observe that the soil moisture process (seen earlier in Figures. 1 and 2) is relatively smooth and slow changing, except at the onset of a rainfall. This suggests that the signal might be sparsely represented if we consider the difference between two adjacent sample values. This motivates the following *difference matrix* M_D:

$$M_D = \begin{bmatrix} -1 & 1 & 0 & \cdots & 0 & 0 \\ 0 & -1 & 1 & \cdots & 0 & 0 \\ 0 & 0 & -1 & \cdots & 0 & 0 \\ \vdots & \cdots & \cdots & \cdots & \vdots & \\ 0 & 0 & 0 & \cdots & -1 & 1 \\ 0 & 0 & 0 & \cdots & 0 & -\gamma \end{bmatrix} \quad (5)$$

Table 1: Comparison of approximate sparsity.

N	Sparsity			
	Garden data		Farm data	
	Ψ_D	Ψ_H	Ψ_D	Ψ_H
64	24.9	1.0	15.4	1.1
128	28.4	1.1	21.0	1.1
256	23.1	1.3	19.8	1.3
512	12.4	1.6	17.2	1.3
1024	7.5	1.8	10.0	1.3
2048	7.0	2.5	10.0	2.0

where the last element $\gamma, 0 < \gamma < 1$, ensures that M_D is invertible.

Ideally, one would like the projection of $\mathbf{x}$ on M_D, $\mathbf{s} = M_D\mathbf{x}$, to be a vector containing many zero/near-zero entries. If this is the case, then the original signal $\mathbf{x}$ can be sparsely represented in the M_D-domain as $\mathbf{x} = M_D^{-1}\mathbf{s}$. In the numerical experiments presented in the next section we will use M_D^{-1} as a choice for the representation basis and denote $\Psi_D = M_D^{-1}$ [2].

The temporal correlation and piece-wise smooth feature of the soil moisture process also suggests that it may be more compactly represented through a Haar (wavelet) transformation M_H. We will thus use $\Psi_H = M_H^{-1}$ as a second choice for the representation basis Ψ in our experiment.

We now check the quality of these two matrix choices against the two criteria outlined earlier. It turns out that neither Ψ_D nor Ψ_H can produce a precisely K-sparse signal for $K \ll N$ (the amount of non-zero elements are above 50% in both cases). However, the resulting $\mathbf{s}$ are approximately K-sparse if we neglect small elements. Table 1 shows the approximate sparsity of Ψ_D and Ψ_H under different scale N, the signal size. Here the entire data set is segmented into signals of size N, and the transformation is applied over each signal. The overall sparsity is calculated as the sum of all entries of the normalized $\mathbf{s}$ with values of at least 0.1, and averaged over all signals. We see that as expected the Haar transform is much more effective than the difference matrix at sparsifying the signal.

We next examine the incoherence between these two representation bases and our measurement matrices. As the notion of coherence is not defined for non-orthogonal matrices, in the following we will use its dual-incoherence to indirectly measure the correlation between the proposed Φ_U (Φ_R) and Ψ_D (Ψ_H). The incoherence of two matrices are measured as follows [21]. Projecting each row of Φ onto the space spanned by the columns of Ψ we get:

$$\zeta_j = (\Psi^T\Psi)^{-1}\Psi^T\phi_j^T, \quad (6)$$

where ϕ_j is the jth row of Φ and ζ_j is the vector of coefficients corresponding to its projection on the space spanned by the columns of Ψ. A measure of the incoherence is then defined as

$$\mathbf{I}(\Phi, \Psi) = \min_{j=1,\cdots,N} \Big[\sum_{i=1}^{N} 1\{\rho_i^j \neq 0\} \Big] \in [1, N], \quad (7)$$

where ρ_i^j is the ith entry of vector ζ_j and $1\{A\}$ is the indicator function: it is 1 when A is true and 0 otherwise. The

[2]A similar operation aiming to sparsify a spatial 2D signal was used in [21], but as mentioned in the introduction it did not lead to very good performance.

Table 2: Comparison of incoherence.

N	$\mathbf{I}(\Phi_R, \cdot)$	
	Ψ_D	Ψ_H
64	63	11
128	125	34
256	255	66
512	512	130
1024	1024	258
2048	2048	514

larger this quantity, the more incoherent the two matrices. In Table 2, we show the incoherence obtained from Equation (7), for the random measurement matrix Φ_R with the two choices of Ψ at different scales. We see Ψ_D has much higher incoherence with our measurement matrix than Ψ_H does. Thus we have two representation bases, one (Ψ_H) better at sparsifying the signal while the other (Ψ_D) much more incoherent with the measurement matrix. In the next section we examine which choice leads to better reconstruction performance.

5. NUMERICAL EXPERIMENTS

In this section we evaluate the effectiveness of using compressive sensing techniques to solve the soil moisture measurement problem using the matrices introduced in the previous section, through extensive numerical experiments. In the remainder of this section, the garden data refers to the surface level (top level) soil moisture process shown in Figure 1, and the farm data refers to the soil moisture process of Node 3 as shown in Figure 2. Unless otherwise specified, we trim the real and simulated data to 4096 observations (or discrete times steps) in total, for the convenience of the experiment. To perform the experiments, we divide each data set into W windows (or signal) of N points each. Our sampling and recovery algorithms are applied to each window separately and similarly. The $N \times 1$ discrete signal within the w-th window ($1 \leq w \leq W$) is denoted as $\mathbf{x}_w$. Within each window, $M < N$ measurements are taken. The goal is to reconstruct $\mathbf{x}_w$ from the M direct observations.

Breaking the data set into windows of N allows us to balance the computational complexity/delay and estimation accuracy. If the measurement and reconstruction is done in a close-to-real time fashion, then it is desirable to perform these operations over a smaller N. On the other hand, larger N generally results in better estimates, though at the expense of increased computational complexity.

The quality of the reconstruction is measured by the following average error criterion:

$$AvgError = \frac{1}{NW} \sum_{w=1}^{W} ||\mathbf{x}_w - \hat{\mathbf{x}}_w||_1 \ , \qquad (8)$$

where W is the number of windows ($W = 4096/N$); $\mathbf{x}_w$ and $\hat{\mathbf{x}}_w$ are the true and estimated signal of window w; $||\mathbf{x}_w - \hat{\mathbf{x}}_w||_1$ is the sum of absolute errors in the estimate. This error is further averaged over 20 random trials when the measurement schedule is generated randomly. The scale-down rate (γ) used in the difference matrix M_D is 0.001. The sampling times under a random schedule (RS) is generated using a uniform probability distribution.

The overall quality of signal reconstruction is determined by three elements: the choice of measurement scheduling matrix Φ, the choice of the representation basis Ψ, and the choice of a recovery algorithm (also referred to as a *solver* below). In the following, we will first examine what types of solvers work best with our choices of Φ (Φ_U and Φ_R) and and Ψ (Ψ_D and Ψ_H). We then compare the performance of different combinations of these matrices.

5.1 Effect of recovery algorithms

We first investigate what CS recovery algorithms or solvers work best with our selection of Φ and Ψ. A candidate list of these algorithms is discussed in Section 3, and they include SL0, IRWLS, OMP and BP (using LP). Of these, SL0 aims to minimize the l_o norm, while the others aim at minimizing the l_1 norm. The Matlab code of IRWLS, OMP, and LP is obtained from Sparse Lab [33] and SL0 from [34].

A set of experiments are run by increasing the window size N. For each window, the number of measurement M is set to 10% of N. As the Haar basis requires N to be a power of two, we set $N = 2^p, p = 6, 7, 8, 9, 10, 11$. For each value of N we evaluate the average estimation error in applying one of the above algorithms to the two data sets while using Φ_R as the measurement matrix, and Ψ_D and Ψ_H respectively as the representation basis. The results are shown in Figure 3. Our main observations are as follows.

Firstly, compared to Haar, the difference matrix Ψ_D shows significant advantage regardless of the data used and the solver used: the $AvgError$ of Ψ_H is at least 10 orders of magnitude higher than Ψ_D. As discussed earlier, Ψ_H sparsifies the data better than Ψ_D, while the later has much higher incoherence with the measurement matrix Φ_R. This observation thus suggests that in this case incoherence is more critical in determining the effectiveness of these solvers.

Secondly, we see that there are substantial performance gaps among different recovery algorithms. When Ψ_D is used, we see from Figure 3(a) and 3(c) that SL0 and LP perform the best (these two curves almost completely overlap) and they significantly outperform IRWLS and OMP. When Ψ_H is used, Figure 3(b) and 3(d) (the two curves of OMP and IRWLS almost completely overlap as well) again show that LP performs the best and significantly so. Furthermore, since the soil moisture content is measured between 10 and 35 (in %), an estimation procedure effectively fails if its $AvgError$ exceeds 10. In this sense except for LP, all other solvers do not work successfully with Ψ_H. These observations suggest that the estimation quality of LP and SL0 is much more robust to the level of sparsity than the faster solvers (OMP, IRWLS) when there is sufficient incoherence (in the case of Ψ_D. At the same time, LP is also robust to weak incoherence when there is sufficient sparsity (in the case of Ψ_H).

Based on these results, for the rest of our numerical evaluation we will limit our attention to SL0 and LP. As LP is more computationally costly than SL0, we will only use SL0 when Ψ_D is used, and LP when Ψ_H is used.

5.2 Effect of measurement matrices

We next study the impact of scheduling methods on the reconstruction quality. The three measurement matrices we examine are random (Φ_R), uniform (Φ_U) and Gaussian (Φ_G) introduced in Section 4.1. Note again that the Gaussian matrix is used as a point of comparison; it is not a practical scheduling policy for our problem.

Figure 4 illustrates the reconstruction quality under these

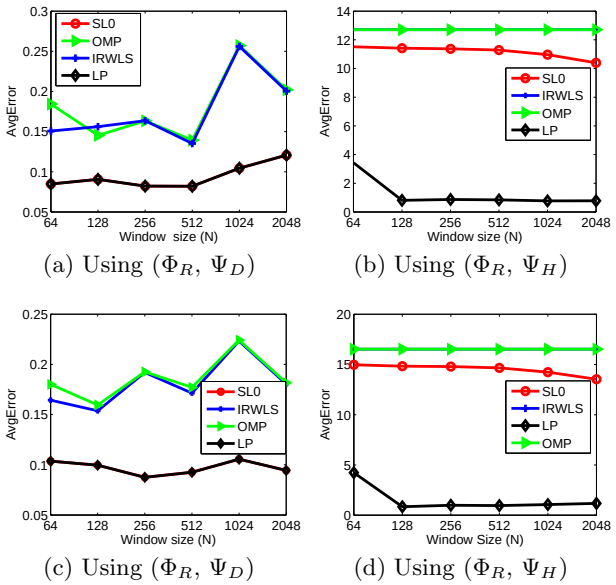

(a) Using (Φ_R, Ψ_D) (b) Using (Φ_R, Ψ_H)

(c) Using (Φ_R, Ψ_D) (d) Using (Φ_R, Ψ_H)

Figure 3: Comparison of reconstruction performance: (a)(b) Garden data; (c)(d) Farm data

three scheduling methods, with respect to the true soil moisture values (denoted as TV in the figure). In this set of results, the representation basis and solver used are Ψ_D and SL0, respectively, the window size is $N = 128$, and the sampling rate is $M = 10\%N$. To observe the finer differences among these methods, Figure 4 also provides zoomed-in views around two peaks in the original data. Overall, all three scheduling methods perform very closely, and all of them reconstruct the original signal to very high accuracy.

To be more precise in quantitative comparison, Table 3 further shows the corresponding *AvgError* calculated over different time segments in the data. Here, a range of "Total" includes the entire period (i.e, from 1 to 4096), while the ranges "Peak1" and "Peak2" refer to the two peaks amplified in Figure 4 within each data set. Peak 1 is given by the time intervals [400, 500] and [600, 750] for the garden and farm data, respectively. Peak 2 is given by the time intervals [3300, 3400] and [2200, 2400] for the garden and farm data, respectively. As a comparison point, we also present the same set of results when the Haar basis matrix Ψ_H and the LP solver are used in same table. We repeat the same calculation at different sampling rates, from 10% to 30%, and present these results in Figure 5.

When the same (Ψ, solver) pair is used, the main factor affecting the final reconstruction performance is the incoherence between Ψ and the measurement matrix Φ. The incoherence between (Φ_R, Φ_U, Φ_G) and Ψ_D is 125, 127, and 128, respectively, at $N = 128$. Thus it is not surprising that we see very close performance as evidenced in Figure 4. In particular, we see that the uniform (periodic) scheduling provides the best overall performance.

It is however interesting to see, from Table 3, that both uniform and random scheduling outperform Gaussian scheduling, especially under the pair (Ψ_D, SL0). This is somewhat surprising, because the Gaussian measurement matrix has the highest incoherence with Ψ_D though by a small amount. This is possibly due to the fact that while in theory Ψ_G should perform the best, such results often rely on the signal being precisely sparse, but in our case the signal $\mathbf{x}$ is only approximately sparsified.

Table 3: Comparison of scheduling methods.

(Ψ, solver)	Data	Range	Φ_R	Φ_U	Φ_G
(Ψ_D, SL0)	Garden	Total	0.0827	0.0623	0.1040
		Peak1	0.8738	0.7682	1.5367
		Peak2	0.2340	0.3795	0.3732
	Farm	Total	0.0909	0.0688	0.1280
		Peak1	0.4712	0.2552	0.3628
		Peak2	0.2156	0.3148	0.4973
(Ψ_H, LP)	Garden	Total	0.8553	0.7537	0.6473
		Peak1	12.9222	0.1744	7.1455
		Peak2	4.2919	4.1016	2.0057
	Farm	Total	0.9797	0.9537	1.3647
		Peak1	2.7720	0.5587	1.8389
		Peak2	4.0324	4.5034	13.3529

5.3 Comparison with interpolation

So far all solvers we tested are taken from the literature on compressive sensing. It is also natural to consider simple interpolation as an alternative to reconstructing the original signal using a small set of samples. In the following we provide an additional comparison point and examine the performance of using spline interpolation (referred to as SP in Figure 6).

In general, spline interpolation is preferred over polynomial interpolation because the interpolation error can be made small even when using low degree polynomials for the spline. Figure 6 illustrates the difference between CS and SP while using the uniform sampling matrix Φ_U. For CS we use Ψ_D as the representation basis and $SL0$ the solver. Clearly, CS performs better than SP, and especially so when the measurement cost (M) and estimation window (N) are low; low values of M and N are preferred as they lead to low computational complexity and estimate delay. However, note that the SP performance is far better than if we had used Ψ_H as the representation basis. This highlights the importance of selecting the right matrix, for otherwise one might do better by simply using standard interpolation.

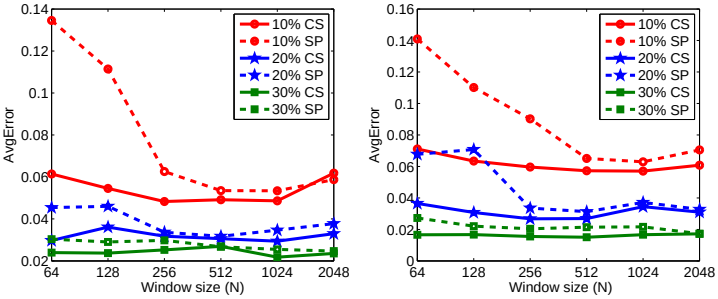

(a) Garden data (b) Farm data

Figure 6: Performance comparison of CS and Spline recovery using Φ_U.

6. CLOSED-LOOP MEASUREMENT SCHEDULING

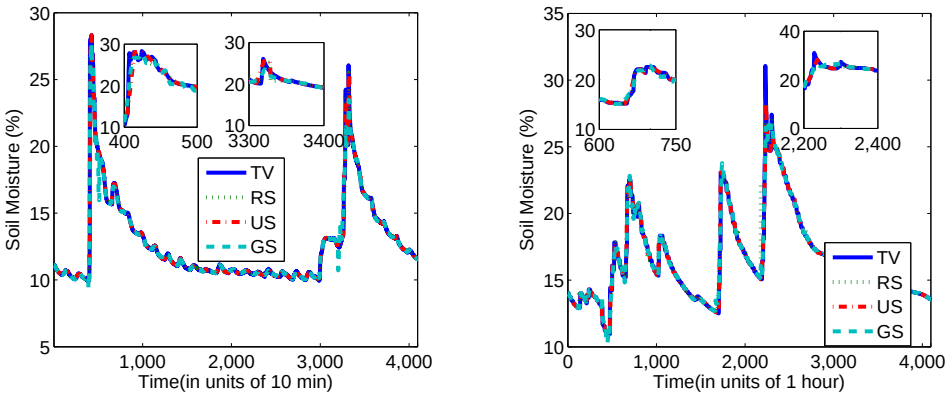

(a) Garden data (b) Farm data

Figure 4: Performance comparison of different scheduling methods, using Ψ_D and SL0.

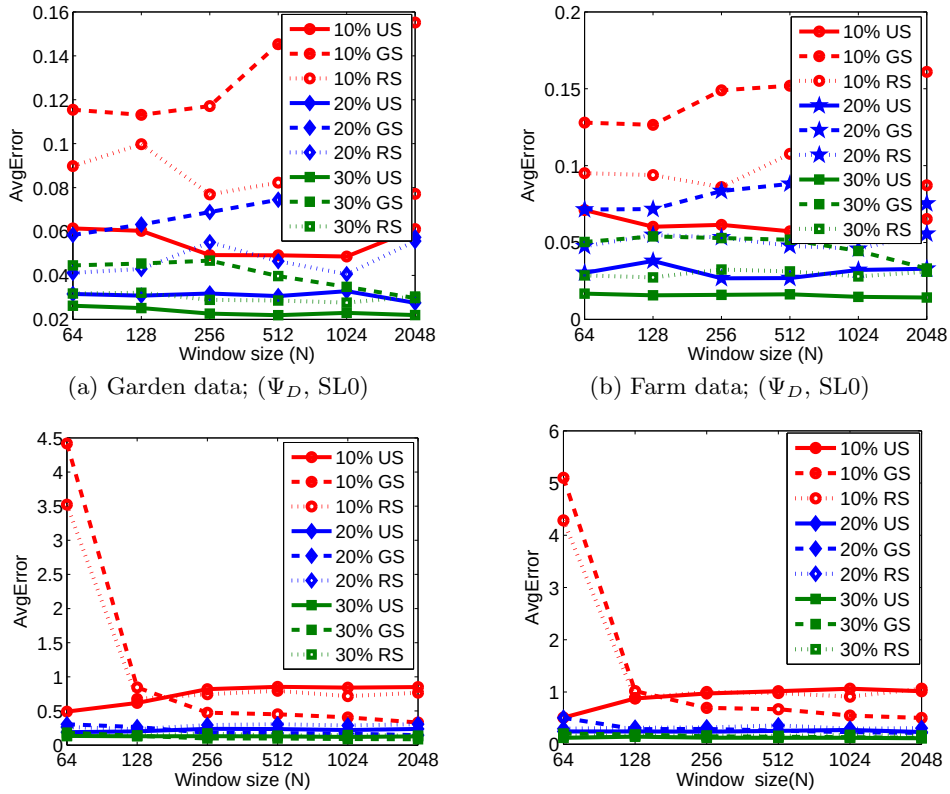

(a) Garden data; (Ψ_D, SL0) (b) Farm data; (Ψ_D, SL0)

(c) Garden data; (Ψ_H, LP) (d) Farm data; (Ψ_H, LP)

Figure 5: Performance comparison of different sampling rate.

As pointed out in the introduction, the type of scheduling policies studied so far (uniform, random, Gaussian) are all open loop ones, i.e., the scheduling decision is independent of the past and current state of the soil moisture process, independent of past scheduling decisions, and does not exploit any physics in the soil moisture dynamics. If one possesses statistical information on the underlying random process, then a conceptually more desirable approach is a closed-loop one, where the physics of the process, as well as the past observations and decisions are taken into account when making the next measurement decision. Note however that unlike the compressive sensing based open-loop approach developed in the preceding section, this closed-loop approach in general requires training in order to learn the statistics from past data. In this section we describe such an approach which formulates a partially observable Markov decision problem (POMDP); more details on this method can be found in [10]. We then compare its performance with compressive sensing based open-loop approach. We further examine whether there is performance gain in combining these two approaches.

Under a closed-loop framework, the soil moisture evolu-

tion (again at a single location) is modeled as a discrete-time stochastic process $\{X_t\}_{t=0,1,2,\ldots}$. A decision U_t, $t = 1, 2, \cdots$, is made at time t: $U_t = 1$ denotes taking a measurement at time t and $U_t = 0$ otherwise. If a measurement is taken, then a perfect observation $Y_t = X_t$ is made at time t, otherwise; a "blank" observation results.

An estimated process $\hat{X}_t$ of the soil moisture is formed, with each new observation, using all past observations (some of which are blanks) and all past scheduling decisions:

$$\hat{X}_t = h_t\big(Y_0, Y_1, \cdots, Y_t; U_1, U_2, \cdots, U_t\big). \tag{9}$$

Similarly, the scheduling decision for time $t+1$ is based on all prior observations and scheduling decisions:

$$U_{t+1} = g_t\big(Y_0, Y_1, \cdots, Y_t; U_1, U_2, \cdots, U_t\big) \in \{0, 1\}. \tag{10}$$

The sequences $\mathbf{h} := \big(h_1, h_2, \cdots\big)$ and $\mathbf{g} := \big(g_1, g_2, \cdots\big)$ are the *estimation* and *scheduling* policies, respectively. The optimal policy pair $(\mathbf{g}^*, \mathbf{h}^*)$ may be derived by adopting a certain cost (or reward) objective; below is an example of an infinite horizon expected discounted cost:

$$(\mathbf{g}^*, \mathbf{h}^*) = \arg\min_{(\mathbf{g},\mathbf{h})} \mathbb{E}^{\mathbf{g},\mathbf{h}}\left\{\sum_{t=1}^{\infty} \alpha^{t-1} \cdot \Big[c(U_t) + \rho\big(X_t, \hat{X}_t\big)\Big]\right\} \tag{11}$$

where $\alpha \in \{0, 1\}$ is the discount factor, $c(U_t)$ is the measurement cost, and $\rho\big(X_t, \hat{X}_t\big)$ is a penalty on estimation error, e.g., the mean squared error. The expectation is over known statistics of the process X_t.

Compared to an open-loop approach, the above closed-loop framework is conceptually precise (it has an explicit and well-defined optimization criterion), and it allows one to adjust the tradeoff between the measurement cost and the estimation error (by for instance introducing weights for the two cost terms). The main disadvantage of such an approach lies in (1) it requires a priori statistical knowledge of $\{X_t\}$, which may only be available through training and is often an approximation, and (2) it may be computationally intractable due to the large state space.

In the experiments below, we will assume $\{X_t\}$ to be first-order Markov, with which the above problem becomes a POMDP. This allows us to limit our attention to the class of Markov policies. We will further assume that X_t can only take on a finite number of values (i.e., soil moisture is quantized), to limit the state space. Specifically, the quantization levels used are given by $Q = [8, 9.5, 11, 12.5, 13.25, 14, 14.75, 15.5, 16, 17.5]$ (all in %).

With these assumptions, the soil moisture data is first quantized, and then the first T quantized values are used as a training set to generate a state transition matrix $\mathbb{P}$ that describes the evolution of the discrete-time discrete-valued process $\{X_t\}$. The POMDP problem defined in Eqn (11) is solved using Cassandra's pomdp-solve package [35]. The cost function $c(U_t)$ is set to 0.05, 0.10, 0.50 and 1.00 for $U_t = 1$ and 0 otherwise in different experiments. This is intended to control the sampling cost. The penalty $\rho()$ is set to be the sum of absolute error. The discount factor (α) is set to 0.99. An interested reader is referred to [10] for more on parameter options. The amount of data in the training set (T) is set to 1000 and 3000, respectively. These are referred to as T1 and T2 in Figure 7, respectively. The solution to (11), in the form of a policy pair is then applied to the segment of garden data [3001, 5888], with the resulting estimation error

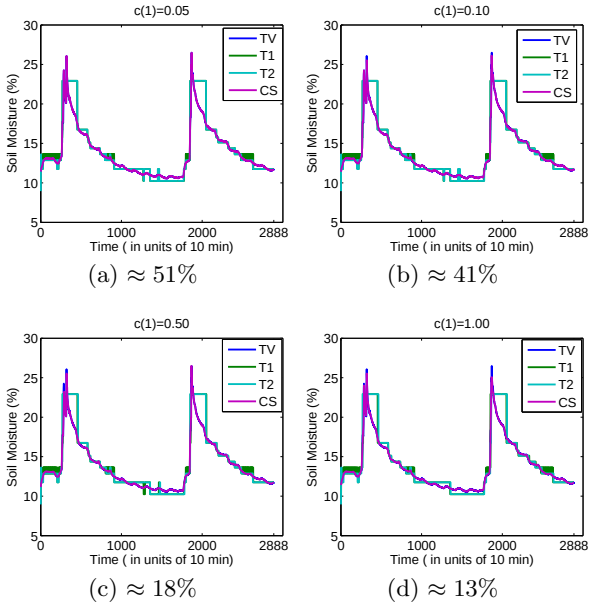

(a) $\approx 51\%$ (b) $\approx 41\%$

(c) $\approx 18\%$ (d) $\approx 13\%$

Figure 7: Performance under different sampling rates.

Table 4: Open-loop vs. closed-loop.

Method	T	Sampling rate (%)	AvgError
$(\Phi_U, \Psi_D$, SL0)	0	51	0.018
$c(1) = 0.05$	1000	51	0.481
	3000	51	0.418
$(\Phi_U, \Psi_D$, SL0)	0	41	0.018
$c(1) = 0.10$	1000	47	0.523
	3000	38	0.460
$(\Phi_U, \Psi_D$, SL0)	0	19	0.040
$c(1) = 0.50$	1000	22	0.652
	3000	17	0.594
$(\Phi_U, \Psi_D$, SL0)	0	13	0.049
$c(1) = 1.00$	1000	16	0.691
	3000	11	0.646

reported in Figure 7 and Table 4. For comparison, we also present results on the same data set (garden data, [3001, 5888]) by using uniform scheduling Φ_U, representation basis Ψ_D and solver SL0, with a window size of $N = 128$.

We see that compressive sensing based reconstruction performs significantly better than the closed-loop approach, under a range of cost levels and sampling rates (the rates cannot be perfectly controlled in the experiments, and are organized into groups of similar values). Furthermore, the open-loop approach improves much faster as the sampling rate increases. The reason for the performance difference, as well as the slow improvement of the closed-loop approach, lies in the fact that in order to be computationally tractable, we had to quantize the soil moisture in solving (11). As a result the output of the estimation/reconstruction is also quantized, which contributed to a significant part of the error; this phenomenon is also visible in Figure 7. We also examine the effect of combining closed-loop scheduling (the output scheduling policy $\mathbf{g}^*$ from (11)), and the reconstruction based on Ψ_D and SL0, i.e., to replace the measurement given by Φ with $\mathbf{g}^*$. The comparison results over the same data segment are shown in Table 5.

Table 5: Closed-loop scheduling, open-loop estimate

Method	T	Sampling rate (%)	$c(1)$	AvgError
$(\Phi_U, \Psi_D$, SL0)	0	11	1.0	0.0763
$(\mathbf{g}^*, \Psi_D$, SL0)	3000	11	1.0	0.0750
$(\Phi_U, \Psi_D$, SL0)	0	17	0.5	0.0533
$(\mathbf{g}^*, \Psi_D$, SL0)	3000	17	0.5	0.0607
$(\Phi_U, \Psi_D$, SL0)	0	37	0.1	0.0241
$(\mathbf{g}^*, \Psi_D$, SL0)	3000	37	0.1	0.0285
$(\Phi_U, \Psi_D$, SL0)	0	51	1.0	0.0191
$(\mathbf{g}^*, \Psi_D$, SL0)	3000	51	1.0	0.0195

We conclude that using closed-loop scheduling adds very little, if any at all, to the reconstruction accuracy. This shows that the compressive sensing method developed in the previous sections performs very well indeed, with relatively little room to improve. It also suggests that the combination of Ψ_D and SL0 is extremely robust to the type of measurement schedules used.

7. CONCLUSION AND FUTURE WORK

In this paper, we considered the problem of monitoring soil moisture evolution using a wireless network of in-situ sensors. We showed that at the cost of small estimation error we can significantly reduce energy consumption by taking a sparser set of measurements. We discussed how to apply compressive sensing techniques to achieve this. With very strict constraints imposed on the measurement matrix, we investigated what types of representation basis can successfully sparsify the soil moisture signal while being sufficiently incoherent with the measurement matrix. We showed that a difference matrix attains a good tradeoff for these objectives. The effectiveness of this combination is validated through extensive numerical experiments over real soil moisture data as well as simulated soil moisture data, and through comparison with the often-used Gaussian measurement matrix and a closed-loop approach. We showed that with these choices we can achieve very low estimation error at no more than 10% of the standard sampling rate.

To give a more concrete sense of how much this level of reduction in sampling rate can ultimately contribute to the overall energy saving in the operation of an entire monitoring system, we quote below some quantities based on a soil moisture monitoring system Ripple-2 developed at the University of Michigan. The design and development of this system have been partially documented in [4]. We estimate that the lifetime of a wireless node under our system implementation would be significantly increased, from around 6 months to nearly 5 years by sampling at an average of 100-min intervals compared to 10-min intervals. This is because the amount of transmitted data is reduced by 10-fold, and nodes can be in sleep mode for much longer periods of time. It however should be cautioned that such quantitative estimates are clearly heavily dependent on other elements of the system design. For instance, in our implementation the uniform sampling method is particularly appealing because the periodic scheduling is extremely easy to implement and amenable to simple sleep scheduling as well.

There are many future directions to pursue. One question is whether it is possible to obtain more precise performance guarantee or a quantitative relationship between estimation error and the sampling rate. A second is whether there are other interesting measurement techniques to explore. For instance, the estimation error under the current scheme is mainly due to the failure in capturing the peak in the signal after a rainfall. Thus the recovery performance can be improved if the sensors can be alerted to the onset of a rainfall. This is in fact feasible in practice through the use of a rain gauge or similar sensors. Such instrumentation can allow the wireless nodes to wake up upon rainfall and start taking measurements. Similarly, one can also set higher sampling rate immediately following the peak and let it gradually decrease while maintaining the same average rate. We are actively working to include these in the next deployment of our system. Finally, joint design of sampling at multiple locations may be beneficial. This is done naturally in a closed-loop approach. Under a compressive sensing framework it would be interesting to combine closed-loop scheduling for multiple locations with CS based recovery and examine its potential benefit.

Acknowledgment

This work was carried out at the University of Michigan as part of the following two projects: "Soil Moisture Smart Sensor Web Using Data Assimilation and Optimal Control" (NASA grant NNX06AD47G) and "Ground Network Design And Dynamic Operation For Near Real-Time Validation of Space-Borne Soil Moisture Measurements" (NASA grant NNX09AE91G), both through the Earth Science Technology Office, Advanced Information Systems Technologies program (AIST). The authors would like to thank other members of the project team: Profs. M. Moghaddam, D. Teneketzis, and D. Entekhabi, and Y. Goykhman, Q. Wang, Y. Liu, A. Silva, M. Burgin, A. Kakhbod, and A. Castillo. The authors would also like to thank the anonymous reviewers for comments and suggestions that greatly helped improve the quality of the paper.

8. REFERENCES

[1] (2006) Nasa strategic plan. [Online]. Available: http://www.nasa.gov/

[2] I. F. Akyildiz, W. Su, Y. Sankarasubramaniam, and E. Cayirci, "A survey on sensor networks," *IEEE Communications Magazine*, vol. 40, no. 8, pp. 102–114, August 2002.

[3] N. Ramanathan, T. Schoellhammer, and E. Kohler, "Suelo: Human-assisted sensing for exploratory soil monitoring studies," in *SenSys'09*, November 2009, pp. 197–210.

[4] M. Moghaddam, D. Entekhabi, Y. Goykhman, K. Li, M. Liu, A. Mahajan, A. Nayyar, D. Shuman, and D. Teneketzis, "A wireless soil moisture smart sensor web using physics-based optimal control: Concept and initial demonstrations," *IEEE Journal of Selected Topics in Applied Earch Observations and Remote Sensing (JSTARS)*, vol. 3, no. 4, pp. 522–535, December 2010.

[5] L. Meier, J. Peschon, and R. M. Dressler, "Optimal control of measurement subsystems," *IEEE Transactions on Automatic Control*, vol. 12, no. 5, pp. 528–536, January 2003.

[6] M. Athans, "On the determination of optimal costly measurement strategies for linear stochastic systems,"

Automatica, vol. 8, no. 1972, pp. 397–412, August 1972.

[7] M. Athans and C. Schweppe, "Optimal waveform design via control theoretic concepts," *Information and Control*, vol. 10, no. 1967, pp. 335–37, October 1967.

[8] H. Kushner, "On the optimum timing of observations for linear control systems with unknown initial state," *IEEE Transactions on Automatic Control*, vol. 9, no. 2, pp. 144–150, April 1964.

[9] M. S. Andersland and D. Teneketzis, "Measurement scheduling for recursive team estimation," *Journal of Optimization Theory and Applications*, vol. 89, no. 3, pp. 615–636, April 1996.

[10] D. Shuman, A. Nayyar, A. Mahajan, Y. Goykhman, K. Li, M. Liu, D. Teneketzis, M. Moghaddam, and D. Entekhab, "Measurement scheduling for soil moisture sensing: From physical models to optimal control," *Proceedings of the IEEE Special Issue on Sensor Networks and Applications*, vol. 98, no. 11, pp. 1918–1933, November 2010.

[11] J. Evans and V. Krishnamurthy, "Optimal sensor scheduling for hidden markov model state estimation," *International Journal of Control*, vol. 74, no. 18, pp. 1737–1742, December 2001.

[12] V. Krishnamurthy, "Algorithms for optimal scheduling and management of hidden markov model sensors," *IEEE Transactions on Signal Processing*, vol. 50, no. 6, pp. 1382–1397, June 2001.

[13] J. S. Baras and A. Bensoussan, "Optimal sensor scheduling in nonlinear filtering of diffusion processes," *SIAM Journal of Control and Optimization*, vol. 27, no. 4, pp. 786–813, July 1989.

[14] L. W. K. Y. Li, E. K. P. Chong, and K. N. Groom, "Approximate stochastic dynamic programming for sensor scheduling to track multiple targets," *Digital Signal Processing*, vol. 19, no. 6, pp. 978–989, December 2009.

[15] E. J. Candés, J. Romberg, and T. Tao, "Robust uncertainty principles: exact signal reconstruction from highly incomplete frequency information," *IEEE Transactions on Information Theory*, vol. 52, no. 4, pp. 489–509, February 2006.

[16] D. Donoho, "Compressed sensing," *IEEE Transactions on Information Theory*, vol. 52, no. 2, pp. 4036–4048, February 2006.

[17] E. Candés and T. Tao, "Near optimal signal recovery from random projections: Universal encoding strategies?" *IEEE Transactions on Information Theory*, vol. 52, no. 12, pp. 5406–5425, December 2006.

[18] D. Baron, M. Wakin, M. Duarte, S. Sarvotham, and R. Baraniuk, "Distributed compressed sensing," *IEEE Transactions on Information Theory*, vol. 52, no. 12, pp. 5406–5425, December 2006.

[19] E. Candés and T. Tao, "Decoding by linear programming," *IEEE Transactions Information Theory*, vol. 51, no. 12, pp. 4203–4215, Decemeber 2006.

[20] Z. Tian and G. Giannakis, "Compressed sensing for wideband cognitive radios," in *Proceedings of IEEE International Conference on Acoustics, Speech and Signal Processing (ICASSP)*, April 2007, pp. 1357–1360.

[21] G. Quer, R. Masiero, D. Munaretto, M. Rossi, J. Widmer, and M. Zorzi, "On the interplay between routing and signal representation for compressive sensing in wireless sensor networks," in *Information Theory and Applications Workshop (ITA 2009)*, February 2009, pp. 206–215.

[22] C. Luo, F. Wu, C. W. Chen, and J. Sun, "Compressive data gathering for large-scale wireless sensor networks," in *Proceedings of the 15th annual international conference on Mobile computing and networking*, September 2009, pp. 145–156.

[23] A. Castillo, "Parallelizing the Distributed Hydrologic Model MOBIDIC," Environmental Engineering,Massachusetts Institute of Technology, Tech. Rep., May 2010.

[24] E. J. Candés, "Compressive sampling," in *Proceedings of the International Congress of Mathematicians*, August 2006, pp. 265–272.

[25] D. L. Donoho, M. Elad, and V. Temlyakov, "Stable recovery of sparse overcomplete representations in the presence of noise," *IEEE Transactions Information Theory*, vol. 52, no. 1, pp. 6–18, January 2006.

[26] E. J. Candés and T. Tao, "Decoding by linear programming," *IEEE Transactions Information Theory*, vol. 51, no. 12, pp. 4203–4215, December 2005.

[27] H. Mohimani, M. Babaie-Zadeh, and C. Jutten, "A fast approach for overcomplete sparse decomposition based on smoothed l0 norm," *IEEE Transactions On Signal Processing*, vol. 57, no. 1, pp. 289–301, January 2009.

[28] D. L. Donoho, "For most large underdetermined systems of linear equations the minimal l1-norm solution is also the sparsest solution," Technology Report, 2004.

[29] (2005) l1-magic: Recovery of sparse signals via convex programming. [Online]. Available: www.acm.caltech.edu/l1magic/downloads/l1magic.pdf.

[30] I. F. Gorodnitsky and B. D. Rao, "Sparse signal reconstruction from limited data using focuss, a re-weighted minimum norm algorithm," *IEEE Transactions on Signal Processing*, vol. 45, no. 3, pp. 600–616, March 1997.

[31] J. A. Tropp and A. C. Gilbert, "Signal recovery from random measurements via orthogonal matching pursuit," *IEEE Transactions on Information Theory*, vol. 53, no. 12, pp. 4655–4666, December 2007.

[32] D. Needell and R. Vershynin, "Signal recovery from inaccurate and incomplete measurements via regularized orthogonal matching pursuit," *IEEE Journal of Selected Topics in Signal Processing*, vol. 4, no. 2, pp. 310–316, February 2010.

[33] (2007) Sparse lab. [Online]. Available: http://sparselab.stanford.edu/

[34] (2008) Sl0. [Online]. Available: http://ee.sharif.ir/ SLzero/

[35] G. E. Monahan, "A survey of partially observable markov decision processes: Theory, models, and algorithms," *Management Science*, vol. 28, no. 1, pp. 1–16, January 1982.